Received: 22 September 2023 | Accepted: 26 January 2024

DOI: 10.1097/HC9.0000000000000419

ORIGINAL ARTICLE

OPEN

Liver-specific mitochondrial amidoxime–reducing component 1 (*Mtarc1*) knockdown protects the liver from diet-induced MASH in multiple mouse models

Yuanjun Guo[1] | Zhengyu Gao[2] | Edward L. LaGory[3] | Lewis Wilson Kristin[4] | Jamila Gupte[2] | Yan Gong[2] | Matthew J. Rardin[5] | Tongyu Liu[6] | Thong T. Nguyen[6] | Jason Long[7] | Yi-Hsiang Hsu[6] | Justin K. Murray[7] | Julie Lade[3] | Simon Jackson[2] | Jun Zhang[2]

[1]Research Biomarkers, Amgen Research, South San Francisco, California, USA

[2]Cardiometabolic Disorders, Amgen Research, South San Francisco, California, USA

[3]Pharmacokinetics and Drug Metabolism, Amgen Research, South San Francisco, California, USA

[4]Translational Safety and Bioanalytical Sciences, Amgen Research, South San Francisco, California, USA

[5]Discovery Technology Platforms, Amgen Research, South San Francisco, California, USA

[6]Center for Research Acceleration by Digital Innovation, Amgen Research, Cambridge, Massachusetts, USA

[7]RNA Therapeutics, Amgen Research, One Amgen Center Drive, Thousand Oaks, California, USA

Correspondence
Simon Jackson, Cardiometabolic Disorders, Amgen Research, 750 Gateway Blvd, South San Francisco, California 94080, USA.
Email: simonj@amgen.com

Abstract

Background: Human genetic studies have identified several mitochondrial amidoxime–reducing component 1 (*MTARC1*) variants as protective against metabolic dysfunction–associated steatotic liver disease. The *MTARC1* variants are associated with decreased plasma lipids and liver enzymes and reduced liver-related mortality. However, the role of mARC1 in fatty liver disease is still unclear.

Methods: Given that mARC1 is mainly expressed in hepatocytes, we developed an N-acetylgalactosamine–conjugated mouse *Mtarc1* siRNA, applying it in multiple in vivo models to investigate the role of mARC1 using multiomic techniques.

Results: In ob/ob mice, knockdown of *Mtarc1* in mouse hepatocytes resulted in decreased serum liver enzymes, LDL-cholesterol, and liver triglycerides. Reduction of mARC1 also reduced liver weight, improved lipid profiles, and attenuated liver pathological changes in 2 diet-induced metabolic dysfunction–associated steatohepatitis mouse models. A comprehensive analysis of mARC1-deficient liver from a metabolic dysfunction–associated steatohepatitis mouse model by metabolomics, proteomics, and lipidomics showed that *Mtarc1* knockdown partially restored metabolites and lipids altered by diet.

Conclusions: Taken together, reducing mARC1 expression in hepatocytes

Abbreviations: ALT, alanine aminotransferase; AMLN, Amylin liver non-alcoholic steatohepatitis diet; AST, aspartate aminotransferase; CDAHFD, choline-deficient, L-amino acid-defined, high-fat diet; Cer, ceramides; Chow, chow diet; GalNAc, N-acetylgalactosamine; HDL-C, HDL- cholesterol; IHC, immunohistochemistry; LC-MS, liquid chromatography-mass spectrometry; LDL-C, LDL-cholestrol; mARC1, mitochondrial amidoxime–reducing component 1; MASH, metabolic dysfunction–associated steatohepatitis; MASLD, metabolic dysfunction–associated steatotic liver disease; PC, phosphatidylcholine; PE, phosphatidylethanolamine; PI, phosphatidylinositol; QC, quality control; siRNA, small interfering RNA; TG, triglyceride.

Supplemental Digital Content is available for this article. Direct URL citations are provided in the HTML and PDF versions of this article on the journal's website, www.hepcommjournal.com.

protects against metabolic dysfunction–associated steatohepatitis in multiple murine models, suggesting a potential therapeutic approach for this chronic liver disease.

INTRODUCTION

Metabolic dysfunction–associated steatotic liver disease (MASLD), previously known as NAFLD, is the major cause of chronic liver disease, which affects about 25% of adults in the United States. The spectrum of pathological changes includes fatty liver, metabolic dysfunction–associated steatohepatitis (MASH), and cirrhosis. The first-line treatment mainly focuses on lifestyle modifications and weight control, and currently, there are no FDA-approved pharmacological therapeutics.[1] Therefore, there is an unmet medical need to identify novel therapeutic targets and treatments.

Mitochondrial amidoxime–reducing component 1 (mARC1) is a molybdenum-containing enzyme[2] located on the mitochondrial outer membrane.[3] The enzyme is known for catalyzing the reduction of N-hydroxylated prodrugs[4] and nitrite.[5] Multiple human genetics studies have determined the strong association of a common missense variant *MTARC1* pA165T with MASLD, including protection against all-cause cirrhosis, and decreased plasma alanine aminotransferase (ALT), LDL-cholesterol (LDL-C), and total cholesterol.[6] *MTARC1* pA165T is also associated with reduced liver-related mortality[7] and severity in pediatric MASLD.[8] However, the impact of this missense variant on protein structure and protein function is debated,[9] and this uncertainty limits our understanding of its protective effects. Two rare, protein-truncating loss-of-function variants of *MTARC1*, pR200Ter,[6] and R305Ter,[10] also showed an association with reduced plasma cholesterol, suggesting the protective effect may be through modulation of mARC1 protein level or protein function.[10] Despite the human genetic evidence, the mechanism of mARC1 in liver lipid homeostasis and its role in MASLD progression have not been adequately studied in vivo.

In this study, we examined the role of hepatocyte mARC1 in MASH progression. We designed a mouse small interfering RNA (siRNA) specifically targeting hepatocytes to investigate mARC1 function in vivo as well as the therapeutic potential of *Mtarc1* knockdown. Knockdown of *Mtarc1* protected the liver from MASLD progression in obese and diet-induced MASH mouse models by reducing liver mass, serum liver enzymes, serum lipids, and liver triglycerides (TG). Lastly, we investigated the underlying mechanism by assessing liver metabolites and protein profiles altered by *Mtarc1* knockdown using a multiomics approach.

METHODS

Liver scRNA-seq analysis and human tissue RNAseq analysis

Processed datasets from Xiong et al[11] and Aizarani et al[12] were downloaded from GEO (https://www.ncbi.nlm.nih.gov/geo), under accession IDs GSE129516 and GSE124395. The quality controls (QC) and analyses were performed using Seurat (v4) R package,[13] following Seurat standard workflow (https://satijalab.org/seurat/articles/sctransform_vignette.html). Raw human RNA-seq datasets for normal tissues were downloaded from GTEx[14] and were processed by Omicsoft based on human genome version GRCh38 and gene model GENCODE v24. Quantification was performed to the gene level based on Omicsoft's implementation of RNA-Seq by Expectation Maximization software package.[15] Gene expression was represented as normalized fragments per kilobase per million reads. Fragments per kilobase per million values were normalized with a refinement of the commonly employed upper-quartile method[16] that sets the fragments per kilobase per million to a value of 10 at the 70th percentile.

Mouse Mtarc1 siRNA design and development

A panel of commercially available siRNA for mouse *Mtarc1* (Dharmacon and Ambion) was screened in vitro to identify active triggers. Two sequence-diverse hits, compounds 1 and 2, with the first nucleotide of the 5' end of the antisense strand at positions 917 and 575 in the full mRNA transcript, respectively, were identified as having potent *Mtarc1* mRNA knockdown activity (data not shown). These siRNA were then prepared in a fully chemically modified format with either a 2'-fluoro or 2'-methoxy substitution in each ribose of the backbone and with incorporation of phosphorothioate internucleotide linkages at the 5' and 3' termini of both strands, and a triantennary N-acetylgalactosamine (GalNAc) moiety was conjugated at the 5' end of each sense strand to facilitate in vivo experimentation with subcutaneous dosing and efficient hepatocellular delivery through interaction with the asialoglycoprotein receptor. (1 antisense: 5' UUCCAUAUAGUGCUUGCUCGG 3', sense: 5' GalNAc3-GAGCAAGCACUAUAUGGAAU-invAb 3';

2 antisense: 5' UCAUUUGCCGAGAACUUCUGG 3', sense: 5' GalNAc3-AGAAGUUCUCGGCAAAUGAU 3', where GalNAc3 indicates triantennary GalNAc and invAb indicates 2'deoxy inverted abasic). Compounds were prepared as reported.[4]

Animal housing and mouse studies

All animal studies involving using mice were approved by the IACUC of Amgen. Ob/ob mice (B6.Cg-Lep ob/J, The Jackson Laboratory #000632) and C57BL/6N (Charles River Laboratories) were single-housed in sterilized cages, fed on chow diet (chow) (Envigo 2920X) or MASH-inducing diet ad libitum. The housing environment is maintained with a 12 h:12 h light/dark cycle, 20°C to 22.2°C, and 34% to 73% humidity.

In 1 diet-induced MASH mouse model, we fed ob/ob mice modified Amylin liver non-alcoholic steatohepatitis diet (AMLN) (Envigo TD.190884) containing 40 kcal% fat, 20 kcal% fructose, and 1.2% cholesterol. In a separate diet-induced MASH model, C57BL/6N mice were fed with the choline-deficient, L-amino acid-defined, high-fat diet (CDAHFD) (Research Diets A06071302) containing 60 kcal% fat with 0.1% methionine and no added choline. Mice were randomized by body weight before any intervention. Blinding was rigorously conducted throughout all studies by using numerical coding. The animal allocation was concealed from the animal house staff and researchers performing the experiments.

Serum and liver collection

Mice were euthanized after 4 hours of fasting. Blood was drawn into serum collection tubes, allowed to clot for 30 minutes at room temperature, and then centrifuged at 10000 rpm for 5 minutes at 4°C. Serum was saved and stored at −80°C. The liver was dissected and preserved either in 10% neutral buffered formalin for histologic examination (Supplemental information, http://links.lww.com/HC9/A848) or snap-frozen in liquid nitrogen for biochemistry or molecular study.

Serum and liver biochemistry analysis

Serum aspartate aminotransferase (AST), ALT, TG, cholesterol, LDL-C, and HDL-cholestrol (HDL-C) were measured using a clinical analyzer (Beckman Coulter). Liver TG was measured using Infinity™ Triglyceride (ThermoFisher Scientific, TR22421) and standard (Pointe Scientific #T7531STD) following the manufacturer's instruction. Liver cholesterol was measured using Infinity™ Cholesterol (ThermoFisher Scientific #TR13421) and cholesterol standard (Pointe Scientific# T7509-STD).

Liver metabolomics analysis

Liver untargeted metabolomic profiling was performed at Metabolon, Inc. (Morrisville, NC, USA) using a combination of liquid chromatography-mass spectrometry (LC-MS) methods as described. Briefly, snap-frozen mouse liver tissue was processed and analyzed by ultrahigh-performance liquid chromatography-tandem mass spectroscopy. The sample was analyzed using 4 different LC-MS methods: acidic positive ion mode conditions with chromatography tailored toward either more hydrophilic or more hydrophobic compounds, basic negative ion mode conditions using a separate dedicated C18 column, and negative ionization mode method coupled with a HILIC column. Raw data processing and statistical analysis were also completed by Metabolon. Briefly, raw data were extracted, peak-identified, and QC processed using Metabolon's hardware and software, followed by curation, metabolite quantification, and data normalization. Welch's 2-sample *t*-test was used to compare the mean between 2 groups in metabolomics analysis performed by Metabolon, Inc.; a *p*-value less than 0.05 is denoted as a significant difference. Pathway enrichment analysis was performed using the Metabolon Client Portal. The enrichment value was calculated as (k/m)/((n−k)/(N−m)), where m = number of metabolites in the pathway, k = number of significant metabolites in the pathway, n = total number of significant metabolites, and N = total number of metabolites.

Liver proteomics analysis

Briefly, snap-frozen liver tissue slices (50–100 mg) were thawed in 2-mL CKMix lysing vials (P000918-LYSK0-A, Bertin Instruments, Rockville, MD) in 300 uL of lysis buffer (100 mM TEAB, 1 mM EDTA, pH 7.5) containing 1 × Halt Phosphatase and protease inhibitor cocktail (78444, ThermoFisher Scientific). Samples were supplemented with 5 µL of benzonase nuclease before homogenizing with a Precellys Evolution Homogenizer (Bertin Instruments, Rockville, MD). The supernatant of homogenates was then reduced, alkylated, and cleaned up using an S-TRAP Mini column (ProtiFi) according to the manufacturer's instructions followed by trypsin/Lys-C (Promega V5073) digestion at 1:50 (wt/wt) overnight at 37°C. Peptides were then dried down by vacuum centrifugation, reconstituted in 50 mM TEAB, and peptide content measured. LC-MS/MS analysis peptides were labeled with TMTpro 18-plex, fractionated offline by high pH reversed-phase liquid chromatography separation, and data were acquired on a Thermo Eclipse tribrid mass spectrometer. Data were searched in Proteome-Discoverer 3.0. Quantification and statistical analysis were carried out using MSstatsTMT,[17] where the differential protein abundance analysis utilized a linear

mixed-effects model. The *p* values were then corrected for multiple hypothesis testing by the Benjamini-Hochberg procedure.[18] Detailed descriptions of sample preparation, mass spectrometric, and chromatographic methods are provided in the Supplemental Information, http://links.lww.com/HC9/A848.

Liver lipidomics analysis

Lipids were extracted from liver tissue using 20 μL 9:1 isopropanol:chloroform+SPLASH II Lipidomix internal standard (Avanti Polar Lipids) per mg tissue. A probe sonicator was used to ensure complete tissue disruption. After sonication, samples were centrifuged at 15,000 × g for 10 minutes at 4°C. Supernatants were transferred to autosamper vial. Small aliquots of each sample were pooled to generate a QC sample for LC-MS/MS–based lipid annotation. Lipid extracts were submitted for LC-MS analysis using a Waters Acquity I-Class ultra-performance liquid chromatography with a Thermo Accucore C30 HPLC column (2.1 × 150 mm, 2.6 μm particle size) using the following mobile phase gradient: Mobile phase A consisted of 60:40 acetonitrile:water + 10 mM ammonium formate + 0.1% formic acid. Mobile phase B consisted of 90:8:2 isopropanol:acetonitrile:water + 10 mM ammonium formate + 1% formic acid. Initial mobile phase composition consisted of 30% mobile phase B, ramped on a linear gradient to 43% B by 5 minutes, 50% B by 5.1 minutes, 70% B by 14 minutes, to 99% B by 21 minutes, held at 99% B until 24 minutes, returned to 30% B for 6 minutes to equilibrate the column. All solvents were LC-MS grade. The mobile phase flow rate was set at 0.35 mL/min. Column temperature was maintained at 40°C throughout the LC run. The ultra-performance liquid chromatography was interfaced with a Thermo Q Exactive HFX mass spectrometer, which was operated in positive/negative polarity switching mode to measure ions in both positive and negative polarity with 60,000 resolution, 1e6 automatic gain control target, 200 ms maximum IT, and scan range of 200–1400 m/z. For lipid annotation, pooled QC samples were subjected to data-dependent MS2 analysis using the same chromatography conditions. For data-dependent MS2, samples were acquired using the MS1 settings described above, while MS2 scans were performed at 30,000 resolution, 1e5 automatic gain control target, 50 ms maximum IT, isolation window of 1.0 m/z, collision energy of 30, and dynamic exclusion of 10 seconds. Data-dependent MS2 annotated lipids were incorporated into a compound database and annotated peaks were integrated using Thermo Tracefinder software. Mass spectrometry results are provided in Supplemental Table 3, http://links.lww.com/HC9/A849. Multiple *t*-tests were performed, with Benjamini, Krieger, and Yekutieli false discovery rate correction of *p*-value for multiple comparisons. False discovery rate-adjusted *p*-value less than 0.05 is denoted as a significant difference. Statistical comparisons of integrated lipids were performed using GraphPad Prism software.

Statistics

For 2 group comparisons, the Mann-Whitney non-parametric test was performed. For multiple comparisons, one-way or two-way ANOVA with post hoc test was performed. *p*-value less than 0.05 is denoted as a significant difference. GraphPad Prism 9 was used for graphing and statistics calculation. All bar graph is presented as mean ± SEM.

RESULTS

MTARC1 is highly expressed in the liver and hepatocytes

To determine an effective approach for targeting mARC1, we first examined *MTARC1* mRNA expression in various human and mouse tissues or cell lines. *MTARC1* expression is relatively abundant in adipose tissue, liver, blood, and some endocrine organs in both humans (Figure 1A) and mice (Figure 1B). This finding is also consistent with human tissue expression profile using human RNAseq data from the Genotype Tissue Expression[14] (Supplemental Figure 1, http://links.lww.com/HC9/A907). We then examined *MTARC1* expression in different cell types in the liver by analyzing liver single-cell RNA-sequencing datasets from humans (GSE129516)[12] and mice (GSE124395).[11] Among multiple cell types, *MTARC1* is highly expressed in hepatocytes, but rarely in nonparenchymal cells or immune cell populations in both human and mouse liver (Figure 1C-F). These findings indicate that mARC1 expression in hepatocytes may be contributing to MASLD and MASH.

Mouse Mtarc1 GalNAc-siRNA conjugate attenuates liver damage in ob/ob mice

N-acetylgalactosamine (GalNAc)–conjugated siRNA delivery has proven to be an effective means to target a gene of interest in hepatocytes.[19] To evaluate mARC1 function in the hepatocyte and fatty liver diseases, we developed tool siRNAs, compounds 1 and 2, from 2 trigger sequences using a chemical modification pattern and a triantennary GalNAc conjugated at the 5' end of each sense strand for hepatocyte uptake. We then tested the knockdown efficiency of the 2 GalNAc-conjugated siRNAs in C57BL/6N mice. The mice were administered a single dose of siRNA at 3 mg/kg s.c., and knockdown was monitored for up to 4 weeks. In mice injected with compound 1, the liver

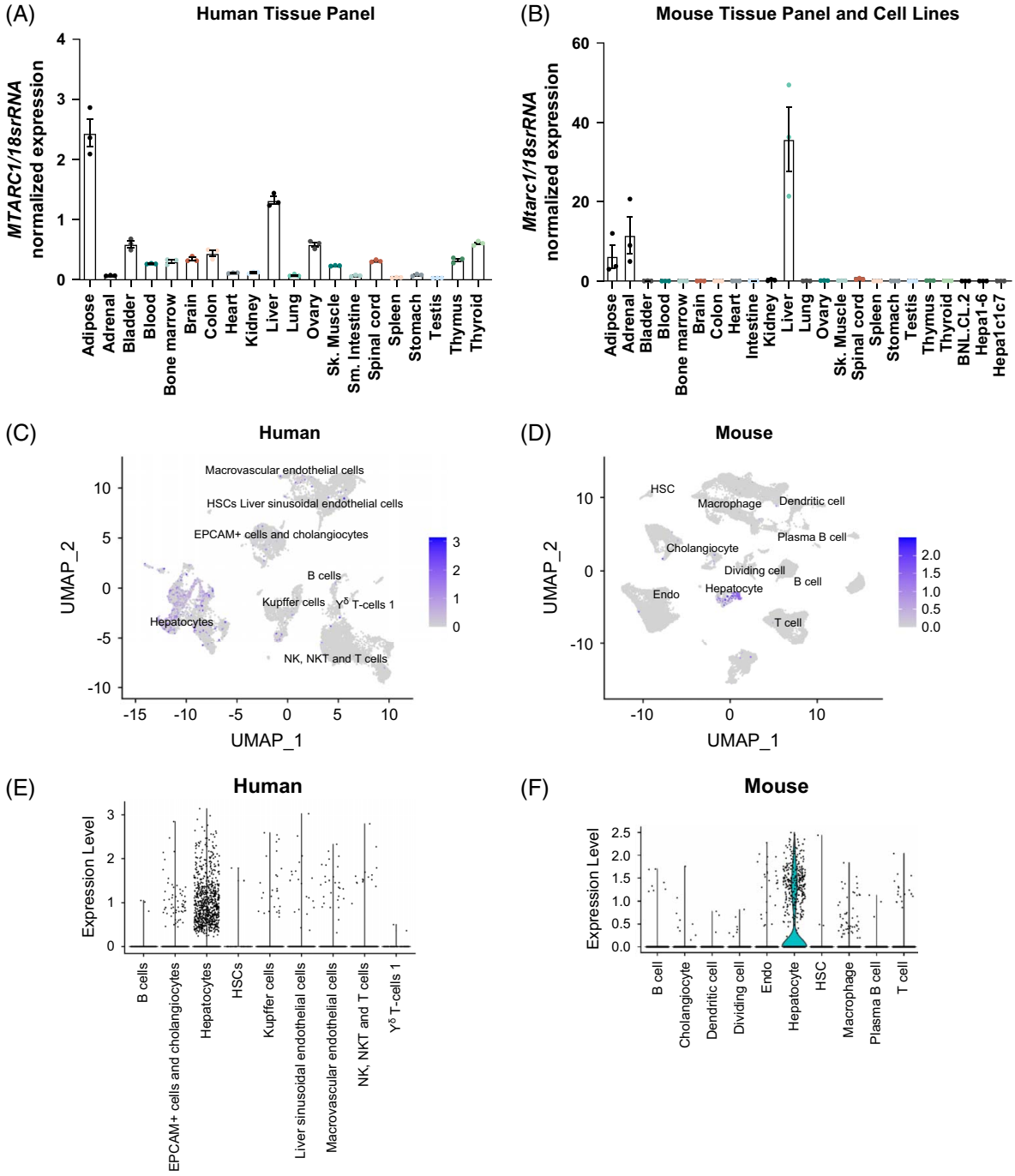

FIGURE 1 Human *MTARC1* and mouse *Mtarc1* expression in various tissues and liver cell types. (A–B) mRNA expression level determined by quantitative real-time PCR (qRT-PCR) in various human tissues (A) or mouse tissues and cell lines (B). *MTARC1* level was normalized to 18srRNA. N = 3 per tissue or cell line. (C–D) UMAP plots of human (GSE124395) (C) and mouse (GSE129516) liver scRNA-seq (D) with a normalized expression of *MTARC1* represented in scale from gray (low) to blue (high). (E–F) Violin plots of normalized expression distribution of *MTARC1* across cell type in humans (GSE124395) (E) and mice (GSE129516) (F). Abbreviations: MTARC1, mitochondrial amidoxime–reducing component 1; UMAP, Uniform Manifold Approximation and Projection.

Mtarc1 mRNA expression level was reduced by more than 80% after 1 and 2 weeks. More than a 50% reduction of *Mtarc1* mRNA gene expression and protein expression was still observed at 4 weeks after injection (Supplemental Figure 2A-2B, http://links.lww.com/HC9/A850, Supplemental Figure 6, http://links.lww.com/HC9/A908). The other candidate, compound 2, reduced the *Mtarc1* mRNA expression by 60% after 1 week of injection, but only 20% after 2 weeks, and no obvious knockdown was observed after 4 weeks after injection (Supplemental Figure 2A, http://links.lww.com/HC9/A850). Therefore, we advanced compound 1 to the additional studies presented here.

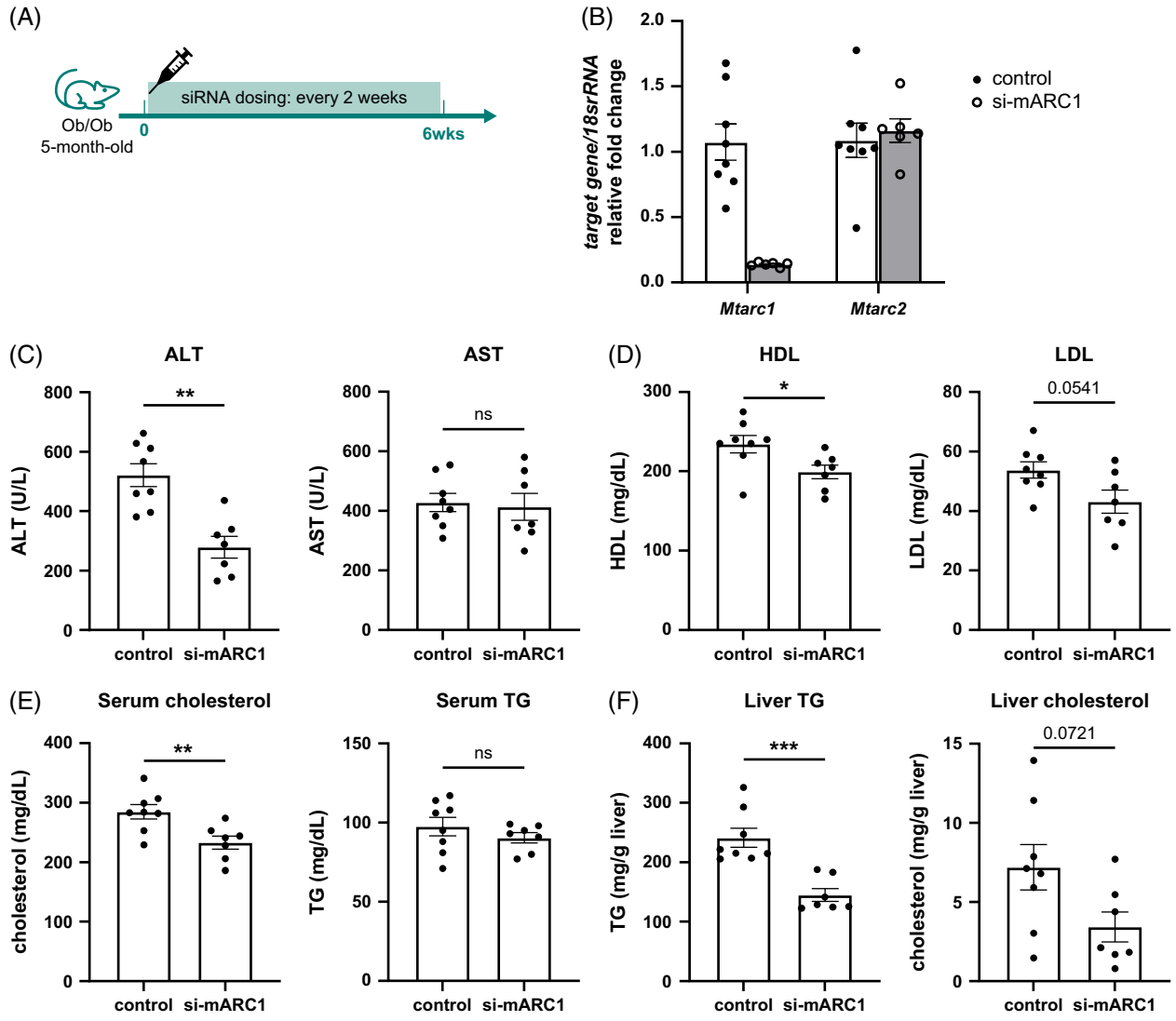

FIGURE 2 *Mtarc1* siRNA protects liver function in ob/ob mice. (A) Schematic diagram of study design. A 5-month-old male ob/ob mice were administered 3 mg/kg *Mtarc1* siRNA (si-mARC1) or vehicle control (control) by subcutaneous injection every 2 weeks for 6 weeks. (B) *Mtarc1* and *Mtarc2* gene expressions in the liver determined by qRT-PCR. (C) Serum ALT and AST levels. (D) Serum lipid profile HDL-C, LDL-C. (E) Serum cholesterol, TG. (F) Liver TG and liver cholesterol level. Data are presented as mean ± SEM, control: n = 8, si-mARC1: n = 7. *$p < 0.05$, **$p < 0.01$, ***$p < 0.001$, ns: not significant, Mann-Whitney test. Abbreviations: ALT, alanine aminotransferase; AST, aspartate aminotransferase; HDL-C: high-density lipoprotein cholesterol; LDL-C: low-density lipoprotein cholesterol; MTARC1, mitochondrial amidoxime–reducing component 1; qRT-PCR, quantitative real-time PCR; TG, triglyceride.

Considering the protective association of *MTARC1* variants on serum lipid levels,[6,7,10] we first examined the effect of *Mtarc1* knockdown in obese mice with disrupted circulating lipids. 5-month-old ob/ob mice were injected with compound 1 (si-mARC1) at 3 mg/kg or vehicle control (control) s.c. every 2 weeks for 6 weeks (Figure 2A). Compared to control, the liver *Mtarc1* mRNA expression was maintained at less than 15% with no effect on *Mtarc2* mRNA expression (Figure 2B). *Mtarc1* knockdown in the liver significantly reduced serum ALT, HDL-C, and total cholesterol levels in ob/ob mice (Figure 2C-E). Liver TG in the *Mtarc1* siRNA group was also significantly decreased by about 20% compared to control (Figure 2F). A nonstatistically significant decrease in serum LDL-C and liver cholesterol by si-mARC1 was also observed (Figure 2D, F). These changes recapitulated the human genetics findings, indicating that hepatocytes are the therapeutic target for mARC1 MASH therapeutics.

Hepatic Mtarc1 knockdown protected ob/ob mice against diet-induced MASH

To examine the effect of *Mtarc1* siRNA in MASH, we fed male ob/ob mice (5–6 wk-old) a modified high-cholesterol,

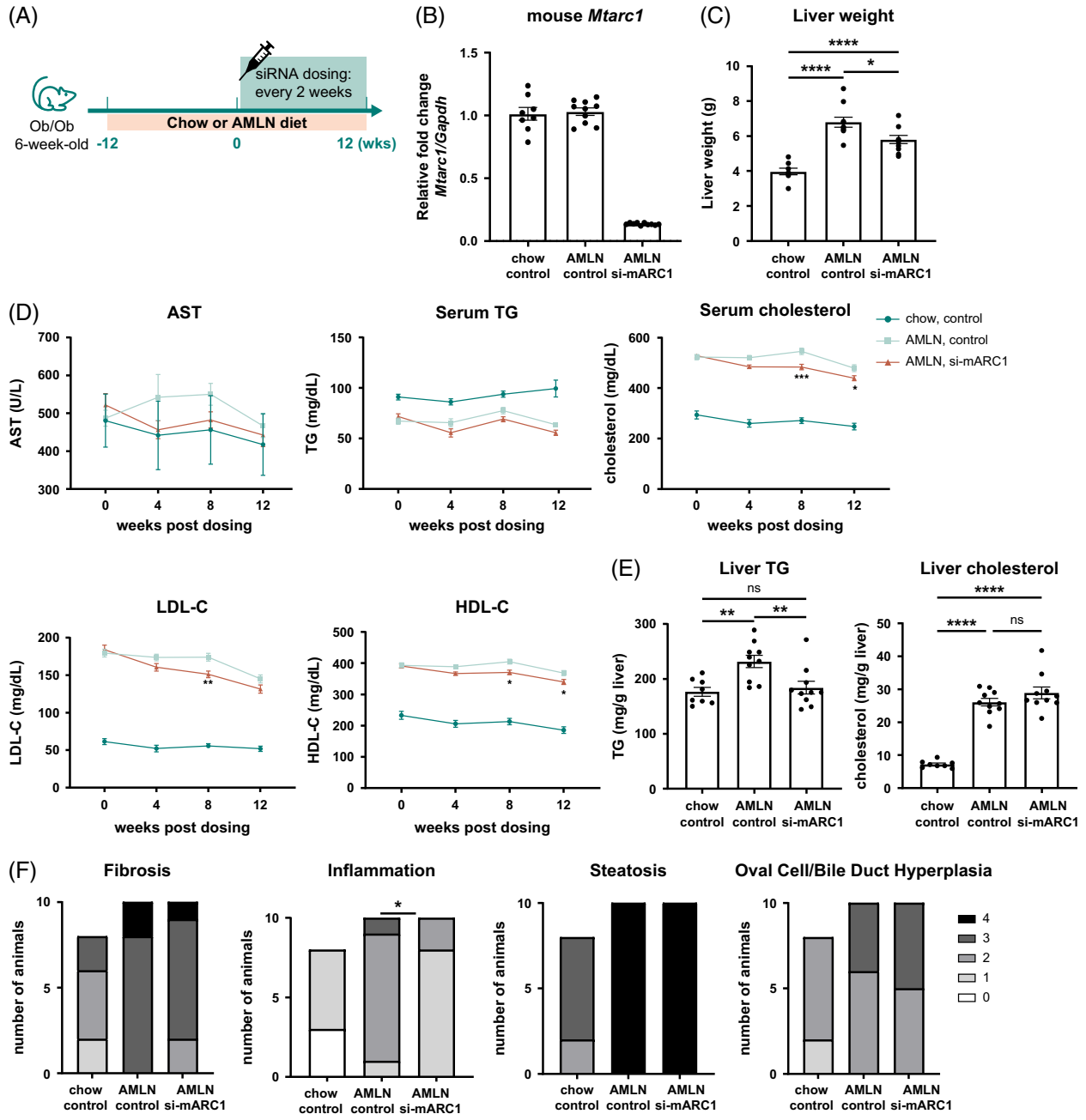

FIGURE 3 Knockdown of *Mtarc1* protects ob/ob mice from a diet-induced liver MASH-like phenotype. (A) Schematic diagram of study design. 6-week-old ob/ob male mice were fed a chow diet or AMLN diet for a total of 24 weeks. After 12 weeks, mice were administered 3 mg/kg *Mtarc1* siRNA s.c. every 2 weeks for 12 weeks. Chow-fed group: n = 8; AMLN-fed groups: n = 10. (B) Liver *Mtarc1* mRNA expression determined by qRT-PCR. (C) Liver weight. (D) Serum transaminase and lipid levels including AST, LDL-C, HDL-C, TG, and cholesterol at 0, 4, 8, and 12 weeks of treatment. (E) Liver TG and cholesterol. Data are presented as mean ± SEM; *$p < 0.05$, **$p < 0.01$, ***$p < 0.001$, ****$p < 0.0001$; C and E using one-way ANOVA with post hoc Tukey test, D using two-way ANOVA with post hoc Tukey test. (F) Histological analysis and quantification, one-way ANOVA with post hoc Kruskal Wallis test. Abbreviations: ALT, alanine aminotransferase; AMLN, Amylin liver MASH; AST, aspartate aminotransferase; HDL-C, high-density lipoprotein cholesterol; LDL-C, low-density lipoprotein cholesterol; MASH, metabolic dysfunction–associated steatohepatitis; MTARC1, mitochondrial amidoxime–reducing component 1; TG, triglyceride.

high-fructose AMLN-inducing diet or chow for a total of 24 weeks. After 12 weeks on a diet when animals started to exhibit characteristics of MASH,[20,21] mice were administered si-mARC1 at 3 mg/kg or vehicle control s.c. every 2 weeks for 12 weeks (Figure 3A). Compared to chow control, liver weight, serum AST, cholesterol, LDL-C, HDL-C, liver TG, and cholesterol increased in AMLN-fed mice, and serum TG decreased (Figure 3C-E). Compared to AMLN control, *Mtarc1* siRNA reduced liver *Mtarc1* mRNA expression by 85% as expected (Figure 3B). At the end of the study, the liver weight in the si-mARC1 group was significantly decreased compared to AMLN controls

(Figure 3C). *Mtarc1* knockdown reduced serum lipids including total cholesterol, HDL-C, LDL-C, and TG levels in a time-dependent manner (Figure 3D). There is no significant difference in body weight between the siRNA knockdown group and the AMLN control group (Supplemental Figure 3A, http://links.lww.com/HC9/A851). The elevated liver TG induced by the AMLN diet was also significantly reduced by *Mtarc1* siRNA (Figure 3E).

To further examine histopathological changes in the liver, sections of the liver were stained with hematoxylin and eosin, Masson's trichrome, collagen I immunohistochemistry (IHC), and alpha-smooth muscle actin IHC. In hematoxylin and eosin-stained slides, there was an increase in steatosis, inflammation, and bile duct/oval cell hyperplasia in AMLN-fed mice compared to chow-fed mice (Supplemental information for grading scheme, http://links.lww.com/HC9/A848). Inflammation in *Mtarc1-siRNA*–treated mice was significantly decreased while steatosis and bile duct/oval cell hyperplasia pathology scores were comparable between the si-mARC1 and AMLN control group (Figure 3F, Supplemental Figure 3B, http://links.lww.com/HC9/A851). Percent collagen area (trichrome and collagen I IHC) and stellate cell activation (alpha-smooth muscle actin IHC), determined by image analysis (see Supplemental information, http://links.lww.com/HC9/A848), were increased in AMLN-fed mice compared to chow-fed mice, and there was a minimal decrease in percent collagen area and stellate cell activation in *Mtarc1*-siRNA–treated mice (Supplemental Figure 3B, http://links.lww.com/HC9/A851). Overall, si-mARC1 alleviated liver damage induced by AMLN diet in ob/ob mice.

Downregulation of Mtarc1 in hepatocytes alleviated the progression of diet-induced MASH in lean mice

To further determine the therapeutic effect of *Mtarc1* siRNA, we induced a MASH phenotype in C57BL/6N mice using a CDAHFD. Mice fed with CDAHFD rapidly develop steatosis in the liver in only one week.[22] Using animals on diet for one week, we administered *Mtarc1* siRNA or vehicle control s.c. every 2 weeks for an additional 6 weeks (Figure 4A). Compared to chow controls, liver weights, serum ALT, AST, and liver TG and cholesterol increased in CDAHFD controls, while serum LDL-C and HDL-C decreased (Figure 4C-E). The *Mtarc1* siRNA reduced liver *Mtarc1* mRNA expression by more than 80% compared to the CDAHFD control group (Figure 4B). Compared to the CDAHFD control, *Mtarc1* knockdown significantly decreased liver weight, serum ALT, AST, LDL-C, and liver TG and cholesterol levels (Figure 4C-E), and no body weight change was observed between the siRNA-administered group and CDAHFD control group (Supplementary 4A, http://links.lww.com/HC9/A852). Serum TG and HDL-C were comparable between the si-mARC1 and CDAHFD control groups (Figure 4D). Histologic examination of hematoxylin and eosin-stained sections showed that there was an increase in steatosis, inflammation, and bile duct/oval cell hyperplasia in CDAHFD-fed mice compared to chow-fed mice. In *Mtarc1*-siRNA–treated mice, there was an NS decrease in fibrosis, inflammation, and bile duct/oval cell hyperplasia pathology scores (Figure 4F). Percent collagen area and stellate cell activation were decreased in *Mtarc1* siRNA-administered mice compared to CDAHFD-fed mice (Figure 4G). In addition, the expression of several inflammation and fibrosis genes was decreased by si-mARC1 (Supplemental Figure 4B, http://links.lww.com/HC9/A852). Taken together, *Mtarc1* knockdown in hepatocytes reduced the severity of CDAHFD-induced MASH.

Multiomic analysis of mouse mARC1-deficient liver in diet-induced MASH

To investigate the underlying mechanism of *Mtarc1* knockdown–mediated protection in MASH, we explored liver metabolite profiles using an untargeted metabolomics approach in chow-fed, CDAHFD-fed control, and CDAHFD-fed si-mARC1-treated mice. Among 1090 metabolites identified, there were 687 annotated metabolites significantly different (fold change $\geq$ 1.2 or $\leq$ 0.83, $p < 0.05$) in CDAHFD-fed compared to chow-fed mice, and 136 metabolites altered by si-mARC1 in CDAHFD-fed mice compared to CDAHFD-fed, vehicle control–treated mice. 111 metabolites were common between the 2 comparisons and presented in a heatmap (Figure 5A-C, Supplemental Table 1, http://links.lww.com/HC9/A856). We further performed metabolite enrichment pathway analysis using metabolites altered by si-mARC1. The top-ranked pathways altered by si-mARC1 treatment included the pentose phosphate pathway, phospholipids metabolism, purine metabolism, nicotinate and nicotinamide metabolism, and fatty acid metabolism. Notably, we observed an increase in several acylcarnitines, 3-hydroxy fatty acids, and acyl CoAs in *Mtarc1*-siRNA–treated livers, consistent with increased fatty acid β-oxidation. In addition, *Mtarc1* siRNA treatment also resulted in elevated phosphatidylcholines (PCs), phosphatidylethanolamine (PEs), and lysophospholipids (Figure 5E). *Mtarc1* knockdown in the liver also rescued some molecules in nicotinate and nicotinamide metabolism. The decrease of nicotinamide ribonucleotide, nicotinamide riboside, and nicotinamide adenine dinucleotide in CDAHFD liver was restored by *Mtarc1* siRNA treatment (Figure 5E).

We also performed quantitative proteomics to examine changes in the liver proteome in response to *Mtarc1* siRNA treatment in the CDAHFD-induced MASH model. mARC1 protein level was significantly decreased by *Mtarc1* siRNA compared to the control, yet there was only a modest change in the total liver proteome

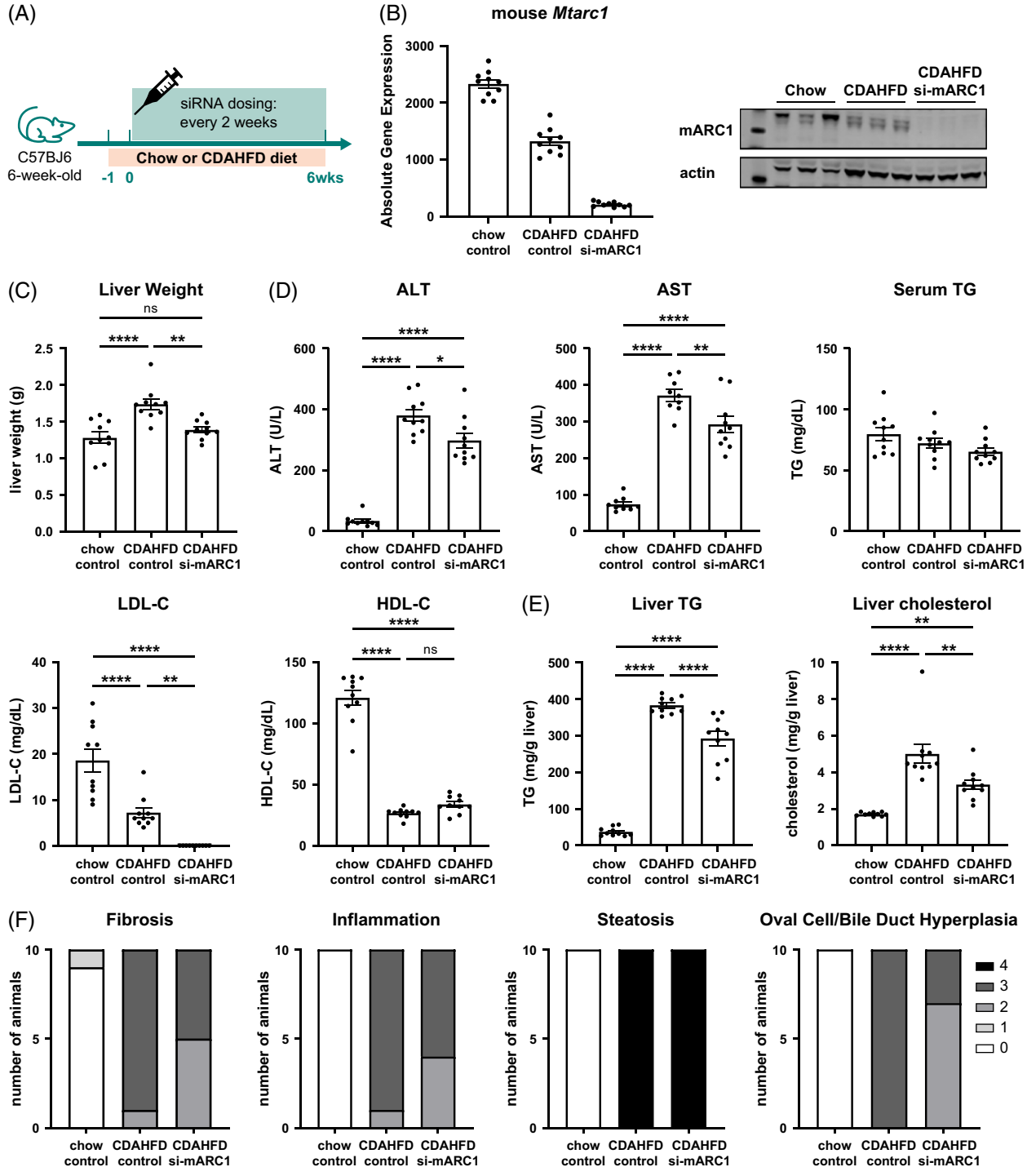

FIGURE 4 *Mtarc1* knockdown protects C57BL6/N mice from a diet-induced liver MASH-like phenotype. (A) Schematic diagram of study design. C57BL6/N mice at 6 weeks of age were fed a chow control diet or CDAHFD diet for a total of 7 weeks. After 1 week on diet, mice were administered 3 mg/kg *Mtarc1* siRNA subcutaneously every 2 weeks for 6 weeks, n = 10 per group. (B) Liver *Mtarc1* mRNA expression determined by qRT-PCR and representative immunoblotting image of mARC1 protein expression in the liver. (C) Liver weight. (D) Serum transaminase and lipid levels including ALT, AST, TG, HDL-C, and LDL-C. (E) Liver TG and liver cholesterol. Data are presented as mean ± SEM, $*p < 0.05$, $**p < 0.01$, $***p < 0.001$, one-way ANOVA with post hoc Tukey analysis. (F) Pathology scores of H&E and trichrome-stained slides. (G) Representative histological images of the liver and quantification of trichrome staining, Col I, and αSMA immunostaining by image analysis. Data are presented as mean ± SEM, $****p < 0.0001$, one-way ANOVA with post hoc Kruskal Wallis test. Black arrow: steatosis; black arrowhead: bile duct/oval cell hyperplasia; blue arrow: fibrosis; blue arrowhead: inflammation; gray arrow: stellate cell activation. Abbreviations: ALT, alanine aminotransferase; AST, aspartate aminotransferase; Col I, collagen I; H&E, hematoxylin and eosin; HDL-C, high-density lipoprotein cholesterol; IHC, immunohistochemistry; LDL-C, low-density lipoprotein cholesterol; MASH, metabolic dysfunction–associated steatohepatitis; MTARC1, mitochondrial amidoxime–reducing component 1; TG, triglyceride; αSMA, alpha-smooth muscle actin.

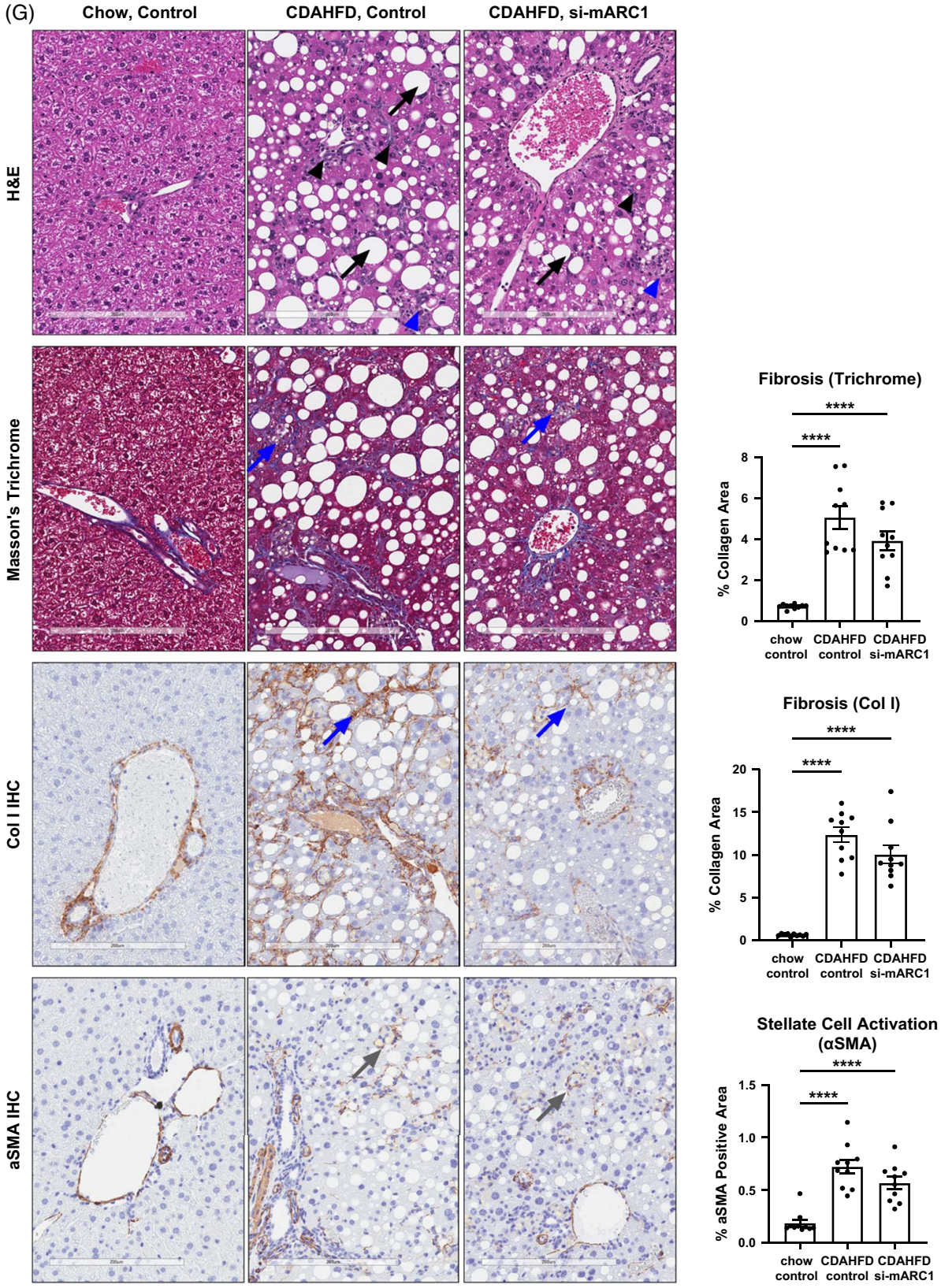

FIGURE 4 *(Continued).*

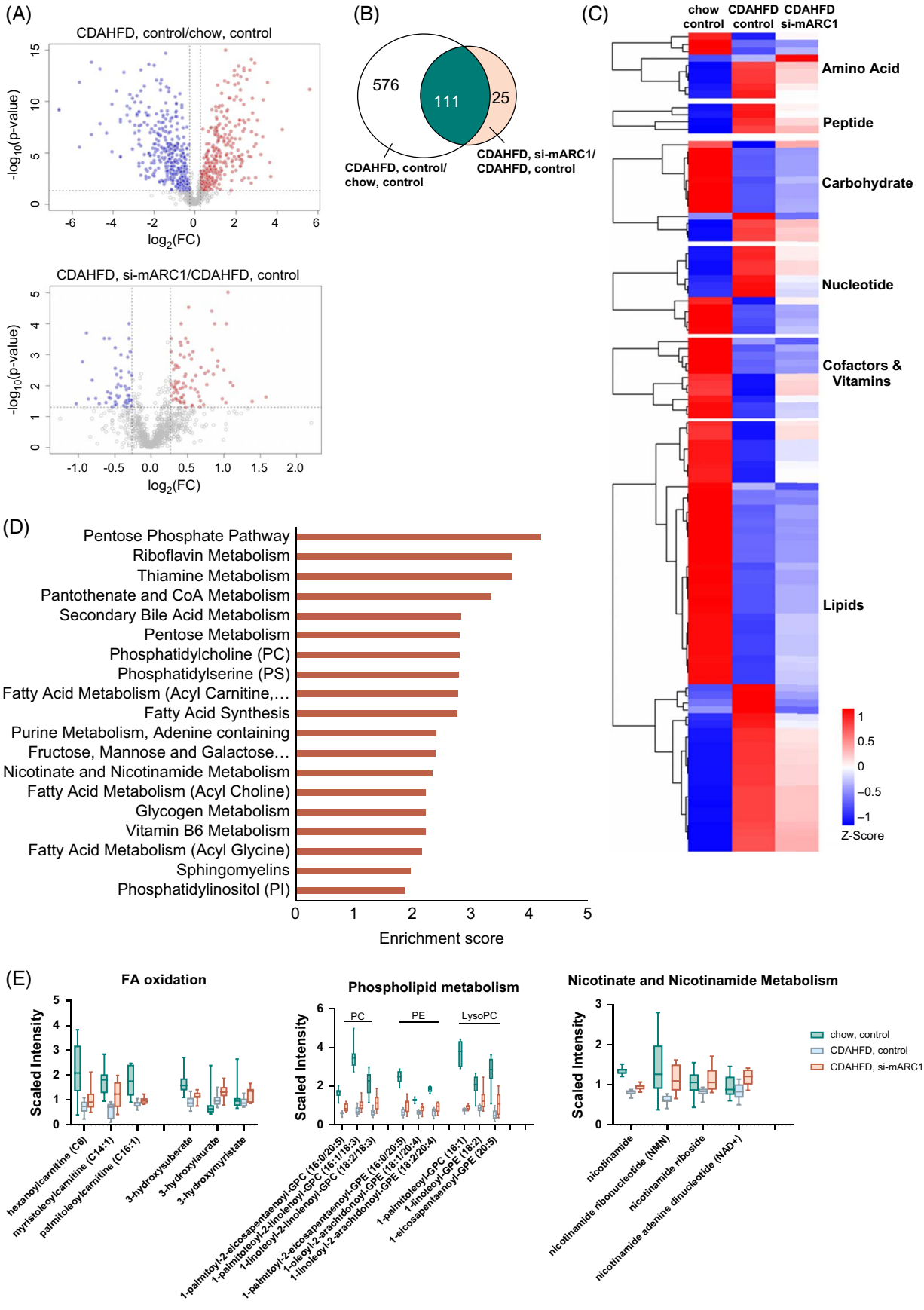

FIGURE 5 Untargeted metabolomics profiling in CDAHFD-induced MASH liver. Untargeted metabolomics was performed using livers collected at the end of 6-week treatment in chow-fed and CDAHFD-fed groups treated with either si-mARC1 or control. n = 10 per group. (A) Volcano

plot depicting $\log_2$(FC) and p values of liver metabolites in CDAHFD, control/chow, control and CDAHFD, si-mARC1/CDAHFD, control. (B) Pie chart of significantly changed metabolites (fold change $\geq$ 1.2 or $\leq$ 0.83, $p < 0.05$) across groups. (C) Heatmap of common metabolites altered in 2 comparisons. (D) Top-ranked metabolic enrichment pathways analyzed by Metabolon Client Portal using the significantly changed metabolites ($p < 0.05$) by si-mARC1. (E) Box plot of representative metabolites. Abbreviations: CDAHFD, choline-deficient, L-amino acid-defined, high-fat diet; FC, fold change; MASH, metabolic dysfunction–associated steatohepatitis; MTARC1, mitochondrial amidoxime–reducing component 1.

(Supplemental Figure 5A, http://links.lww.com/HC9/A853, Supplemental Table 2, http://links.lww.com/HC9/A854). Ingenuity Pathway Analysis using significantly changed proteins (Benjamini-Hochberg adjusted $p < 0.05$, $|\log_2$fold-change$| > 0.5$) also suggested activated oxidation of fatty acids (Supplemental Figure 5B, http://links.lww.com/HC9/A853). Consistent with our metabolomics results, DAVID pathway analysis of significantly changed proteins indicated enrichment of biological processes in lipid metabolism, steroid metabolism, and fatty acid metabolism (Supplemental Figure 5C, http://links.lww.com/HC9/A853).

Since *Mtarc1* knockdown resulted in robust changes in liver lipids and enrichment in lipid metabolism-related pathways, we further delineated the liver lipid profile by untargeted lipidomics using liver tissues from the CDAHFD-induced MASH model. Overall, we identified 727 lipids across 23 lipid classes (Figure 6A, Supplemental Table 3, http://links.lww.com/HC9/A849). The CDAHFD caused major changes in hepatic lipid content, including increases in TGs, diacylglycerols, phosphatidylglycerols, carnitines, and cholesterol esters and decreases in many PCs and lyso-PCs (Figure 6A-B). These observed changes are broadly consistent with human MASLD and MASH.[23,24] In general, many of the diet-induced changes in hepatic lipid content were attenuated by *Mtarc1* siRNA treatment (Figure 6B). TGs and diacylglycerols accounted for many of the lipids that were most downregulated by *Mtarc1* siRNA treatment in CDAHFD-fed mice, while phospholipids, including PEs and N-methyl PEs, were among the most upregulated lipids by *Mtarc1* siRNA treatment (Figure 6B-C). Consistent with the metabolomics findings, decreased PCs were partially restored with *Mtarc1* knockdown. We observed a significant correlation between the chow and *Mtarc1* siRNA treatment, indicating that *Mtarc1* siRNA treatment causes some normalization of TG dysregulation caused by the CDAHFD (Figure 6D). Across the annotated TGs, *Mtarc1* knockdown resulted in a reduction of very long chain, highly saturated TGs, but has only a minor effect on polyunsaturated fatty acids (Figure 6E). In summary, liver lipidomics analysis supports a role of mARC1 suppression in partial normalization of lipidomic profiles of mice on a MASH-inducing diet.

DISCUSSION

The human *MTARC1* variants exhibited a unique protective phenotype different from other known MASH-related variants.[25,26] The carriers showed reduced liver fat on imaging, and lower plasma LDL, but increased HDL and plasma TG. Therefore in this study, we aimed to decipher the protective effects of mARC1 variants and understand how hepatic mARC1 regulated liver metabolism in MASH. Our in vivo studies using obese and diet-induced MASH mouse models demonstrated the protective role of hepatocyte-specific *Mtarc1* knockdown in fatty livers across multiple preclinical models. Importantly, hepatic *Mtarc1* knockdown in mouse models phenocopied the human protective variants.

To understand as yet unclear effect of mARC1 on liver lipid metabolism, for the first time, we delineated the metabolite and lipid landscape of a diet-induced MASH mouse liver rescued by *Mtarc1* siRNA using untargeted metabolomics and lipidomics. In fatty liver diseases, TGs accumulate in the hepatocytes and exacerbate disease progression. Our study showed that *Mtarc1* knockdown dramatically reduced liver TGs in different mouse models, consistent with a recent report.[27] In particular, the reduction of liver TG induced by *Mtarc1* knockdown was characterized by a decrease of very long–chain saturated fatty acids, but not polyunsaturated fatty acids. Since the major source of polyunsaturated fatty acids is from the diet, the decrease of TG containing very long chain, highly saturated fatty acids could be consistent with reduced de novo lipogenesis and acyl chain elongation.

In this study, the liver metabolomic and lipidomic study identified that decreased PC in the CDAHFD-induced liver was mostly reversed by *Mtarc1* knockdown. PC is the major phospholipid in mammalian cells. It is not only the key composition of organelle membranes but also essential in multiple cellular processes and signaling pathways.[28] Studies showed that the level of PCs is decreased in patients with MASH. Meanwhile, PC adjunct therapies have shown effectiveness in the improvement of steatosis, liver enzymes, and metabolic comorbidities in patients with MASLD.[29–31] Importantly, this protective change by *Mtarc1* knockdown in the liver is consistent with increased hepatic polyunsaturated PCs in the human A165T carriers.[32] In addition, increased N-methyl-PE species were observed in the lipidomics analysis, which may indicate that some PC production occurred via the phosphatidylethanolamine N-methyltransferase pathway. Taken together, our findings suggest that *Mtarc1* knockdown in the hepatocyte improved lipid metabolism modulated in MASH. The data also suggest the potential of *Mtarc1* knockdown as an approach to treat MASH or as a combination therapy to improve lipid homeostasis in fatty livers.

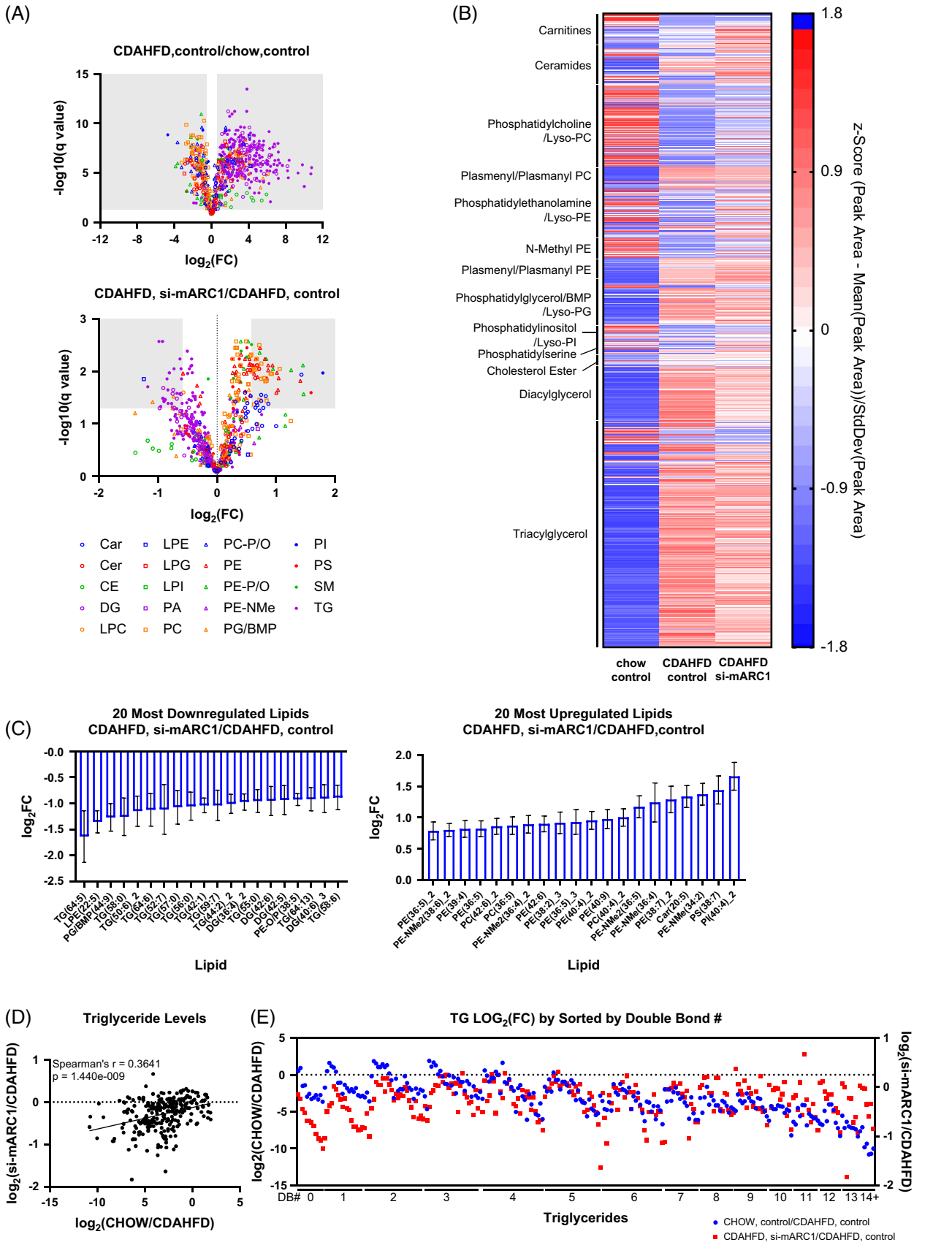

FIGURE 6 Untargeted lipidomics in CDAHFD-induced MASH liver. (A) Volcano plots depicting $\log_2$(FC) and FDR q-values of lipids extracted from livers of chow-fed, and control or mARC1 siRNA-treated mice fed CDAHFD. Fold changes were calculated between CDAHFD/Chow and CDAHFD+si-mARC1/CDAHFD, n = 9–10 per group. (B) Heatmap represents z-scores from liver lipidomics data from mice fed a chow diet or

CDAHFD diet and treated with or without *Mtarc1* siRNA. (C) The top 20 most upregulated and downregulated lipids in *Mtarc1*-siRNA–treated mice fed the CDAHFD diet compared to control mice fed the CDAHFD diet. Top lipids were filtered for significance according to FDR 5% to correct for multiple comparisons and only significantly altered lipids are included. (D) Spearman's correlation analysis for fold change between Chow/CDAHFD and CDAHFD+si-mARC1/CDAHFD groups. (E) Triglyceride species fold change (Chow/CDAHFD; CDAHFD+si-mARC1/CDAHFD) ordered by triglyceride fatty acyl double bond number. Abbreviations: CDAHFD, choline-deficient, L-amino acid-defined, high-fat diet; Car, carnitines; Cer, ceramides; CE, cholesterol esters; DG, diacylglycerol; FC, fold change; FDR, false discovery rate; LPC, lysophosphatidylcholine; LPE, lysophosphatidylethanolamine; LPG, lysophosphatidylglycerol; LPI, lysophosphatidylinositol; PA, phosphatidic acid; PC, phosphatidylcholine; PC-*P/O*, plasmenyl PC; PE, phosphatidylethanolamine; PE-*P/O*, plasmenyl PE; PE-NMe, N-methyl phosphatidylethanolamine; PG/BMP, phosphatidylglycerol/bis(monoacylglycerol)phosphate; PI, phosphatidylinositol; PS, phosphatidylserine; SM, sphingomyelin; TG, triglycerides.

It is important to note that while *Mtarc1* siRNA treatment was able to significantly reduce hepatic TG content and partially revert the liver lipidomic profile, the steatosis score was not significantly different with *Mtarc1* siRNA treatment. It is possible that a longer duration of mARC1 suppression could be needed to fully normalize the hepatic lipid profiles of mice on MASH-inducing diets. Further investigations will be needed to fully understand the extent to which mARC1 suppression can normalize hepatic neutral lipid content and steatosis in MASLD and MASH.

Since mARC1 is known as a reductase located on the mitochondrial outer membrane, further studies are needed to investigate how mARC1 directly affects mitochondrial lipid metabolism, lipid transport,[27] and mitochondrial function. Another aspect that should not be overlooked is that mARC1 is also highly expressed in adipose tissue, where the body stores TGs and regulates lipid and glucose homeostasis. It would be critical to determine mARC1 and *MTARC1* A165T function in the adipocyte using appropriate tissue or cell-specific mouse models.

In summary, *Mtarc1* knockdown in liver hepatocytes resulted in reduced serum transaminases, serum lipids, and liver TG as well as improved liver pathology in obese mice and diet-induced MASH mouse models. Further studies are required to better understand the underlying mechanism of mARC1 in MASH progression and develop potential targeted therapies for MASH.

ACKNOWLEDGMENTS

The authors thank Yingwu Li for the immunohistochemistry staining and image analysis. They also thank Dr. Andrew Schwab at Metabolon Inc. for the analysis and discussion on metabolomics data.

FUNDING INFORMATION

This work is supported by Amgen.

CONFLICTS OF INTEREST

Jun Zhang is currently employed by Septerna Inc. Thong T. Nguyen is currently employed by Meta Platforms, Inc. Yi-Hsiang Hsu is currently employed by HSL Marcus Institute for Aging Research and Harvard Medical School. All authors are or used to be shareholders of Amgen Inc. at the time this work was conducted. The remaining authors have no conflicts to report.

REFERENCES

1. Rinella ME, Neuschwander-Tetri BA, Siddiqui MS, Abdelmalek MF, Caldwell S, Barb D, et al. AASLD practice guidance on the clinical assessment and management of nonalcoholic fatty liver disease. Hepatology. 2023;77:1797–35.
2. Havemeyer A, Bittner F, Wollers S, Mendel R, Kunze T, Clement B. Identification of the missing component in the mitochondrial benzamidoxime prodrug-converting system as a novel molybdenum enzyme*. J Biol Chem. 2006;281:34796–802.
3. Klein JM, Busch JD, Potting C, Baker MJ, Langer T, Schwarz G. The mitochondrial amidoxime-reducing component (mARC1) is a novel signal-anchored protein of the outer mitochondrial membrane. J Biol Chem. 2012;287:42795–803.
4. Gruenewald S, Wahl B, Bittner F, Hungeling H, Kanzow S, Kotthaus J, et al. The fourth molybdenum containing enzyme mARC: Cloning and involvement in the activation of N-hydroxylated prodrugs. J Med Chem. 2008;51:8173–7.
5. Sparacino-Watkins CE, Tejero J, Sun B, Gauthier MC, Thomas J, Ragireddy V, et al. Nitrite reductase and nitric-oxide synthase activity of the mitochondrial molybdopterin enzymes mARC1 and mARC2. J Biol Chem. 2014;289:10345–58.
6. Emdin CA, Haas ME, Khera AV, Aragam K, Chaffin M, Klarin D, et al. A missense variant in Mitochondrial Amidoxime Reducing Component 1 gene and protection against liver disease. PLoS Genet. 2020;16:e1008629.
7. Schneider CV, Schneider KM, Conlon DM, Park J, Vujkovic M, Zandvakili I, et al. A genome-first approach to mortality and metabolic phenotypes in MTARC1 p.Ala165Thr (rs2642438) heterozygotes and homozygotes. Med (N Y). 2021;2:851–863 e853.
8. Hudert CA, Adams LA, Alisi A, Anstee QM, Crudele A, Draijer LG, et al. Variants in mitochondrial amidoxime reducing component 1 and hydroxysteroid 17-beta dehydrogenase 13 reduce severity of nonalcoholic fatty liver disease in children and suppress fibrotic pathways through distinct mechanisms. Hepatol Commun. 2022;6:1934–48.
9. Struwe MA, Clement B, Scheidig A. Letter to the editor: The clinically relevant MTARC1 p.Ala165Thr variant impacts neither the fold nor active site architecture of the human mARC1 protein. Hepatol Commun. 2022;6:3277–8.
10. Sveinbjornsson G, Ulfarsson MO, Thorolfsdottir RB, Jonsson BA, Einarsson E, Gunnlaugsson G, et al. Multiomics study of nonalcoholic fatty liver disease. Nat Genet. 2022;54:1652–63.
11. Xiong X, Kuang H, Ansari S, Liu T, Gong J, Wang S, et al. Landscape of intercellular crosstalk in healthy and NASH liver revealed by single-cell secretome gene analysis. Mol Cell. 2019;75:644–660 e645.
12. Aizarani N, Saviano A, Sagar, Mailly L, Durand S, Herman JS, et al. A human liver cell atlas reveals heterogeneity and epithelial progenitors. Nature. 2019;572:199–204.
13. Hao Y, Hao S, Andersen-Nissen E, Mauck WM, Zheng S, Butler A, et al. Integrated analysis of multimodal single-cell data. Cell. 2021;184:3573–587 e3529.
14. Consortium GT, Laboratory DA, Coordinating Center -Analysis Working G, et al. Genetic effects on gene expression across human tissues. Nature. 2017;550:204–13.

15. Li B, Dewey CN. RSEM: Accurate transcript quantification from RNA-Seq data with or without a reference genome. BMC Bioinformatics. 2011;12:323.
16. Robinson MD, Oshlack A. A scaling normalization method for differential expression analysis of RNA-seq data. Genome Biol. 2010;11:R25.
17. Huang T, Choi M, Tzouros M, Golling S, Pandya NJ, Banfai B, et al. MSstatsTMT: statistical detection of differentially abundant proteins in experiments with isobaric labeling and multiple mixtures. Mol Cell Proteomics. 2020;19:1706–23.
18. Hochberg Y, Benjamini Y. More powerful procedures for multiple significance testing. Stat Med. 1990;9:811–8.
19. Springer AD, Dowdy SF. GalNAc-siRNA conjugates: Leading the way for delivery of RNAi therapeutics. Nucleic Acid Ther. 2018; 28:109–18.
20. Kristiansen MNB, Veidal SS, Rigbolt KTG, Tølbøl KS, Roth JD, Jelsing J, et al. Obese diet-induced mouse models of non-alcoholic steatohepatitis-tracking disease by liver biopsy. World J Hepatol. 2016;8:673–84.
21. Trevaskis JL, Griffin PS, Wittmer C, Neuschwander-Tetri BA, Brunt EM, Dolman CS, et al. Glucagon-like peptide-1 receptor agonism improves metabolic, biochemical, and histopathological indices of nonalcoholic steatohepatitis in mice. Am J Physiol Gastrointest Liver Physiol. 2012;302:G762–772.
22. Sugasawa T, Ono S, Yonamine M, Fujita S, Matsumoto Y Aoki K, et al. One Week of CDAHFD induces steatohepatitis and mitochondrial dysfunction with oxidative stress in. Liver *Int J Mol Sci*. 2021;22:5851.
23. Vvedenskaya O, Rose TD, Knittelfelder O, Palladini A, Wodke JAH, Schuhmann K, et al. Nonalcoholic fatty liver disease stratification by liver lipidomics. J Lipid Res. 2021;62:100104.
24. Ooi GJ, Meikle PJ, Huynh K, Earnest A, Roberts SK, Kemp W, et al. Hepatic lipidomic remodeling in severe obesity manifests with steatosis and does not evolve with non-alcoholic steatohepatitis. J Hepatol. 2021;75:524–35.
25. Mann JP, Pietzner M, Wittemans LB, Rolfe EDL, Kerrison ND, Imamura F, et al. Insights into genetic variants associated with NASH-fibrosis from metabolite profiling. Hum Mol Genet. 2020; 29:3451–63.
26. Du X, DeForest N, Majithia AR. Human genetics to identify therapeutic targets for NAFLD: Challenges and opportunities. Front Endocrinol (Lausanne). 2021;12:777075.
27. Lewis LC, Chen L, Hameed LS, Kitchen RR, Maroteau C, Nagarajan SR, et al. Hepatocyte mARC1 promotes fatty liver disease. JHEP Reports. 2023;5:100693.
28. van der Veen JN, Kennelly JP, Wan S, Vance JE, Vance DE, Jacobs RL. The critical role of phosphatidylcholine and phosphatidylethanolamine metabolism in health and disease. Biochimica et Biophysica Acta (BBA) - Biomembranes. 2017; 1859 (9, Part B):1558–72.
29. Maev IV, Samsonov AA, Palgova LK, Pavlov CS, Shirokova EN, Vovk EI, et al. Effectiveness of phosphatidylcholine as adjunctive therapy in improving liver function tests in patients with non-alcoholic fatty liver disease and metabolic comorbidities: Real-life observational study from Russia. BMJ Open Gastroenterol. 2020;7:e000368.
30. Maev IV, Samsonov AA, Palgova LK, Pavlov CS, Vovk EI, Shirokova EN, et al. Effectiveness of phosphatidylcholine in alleviating steatosis in patients with non-alcoholic fatty liver disease and cardiometabolic comorbidities (MANPOWER study). BMJ Open Gastroenterology. 2020;7:e000341.
31. Osipova D, Kokoreva K, Lazebnik L, Golovanova E, Pavlov C, Dukhanin A, et al. Regression of liver steatosis following phosphatidylcholine administration: A review of molecular and metabolic pathways involved. Front Pharmacol. 2022;13: 797923.
32. Luukkonen PK, Juuti A, Sammalkorpi H, Penttilä AK, Orešič M, Hyötyläinen T, et al. MARC1 variant rs2642438 increases hepatic phosphatidylcholines and decreases severity of non-alcoholic fatty liver disease in humans. J Hepatol. 2020;73: 725–6.

How to cite this article: Guo Y, Gao Z, LaGory EL, Kristin LW, Gupte J, Gong Y, et al. Liver-specific mitochondrial amidoxime–reducing component 1 (*Mtarc1*) knockdown protects the liver from diet-induced MASH in multiple mouse models. Hepatol Commun. 2024;8:e0419. https://doi.org/10.1097/HC9.0000000000000419